iScience

CellPress
OPEN ACCESS

Article

Empirical evidence on the impact of urban overheating on building cooling and heating energy consumption

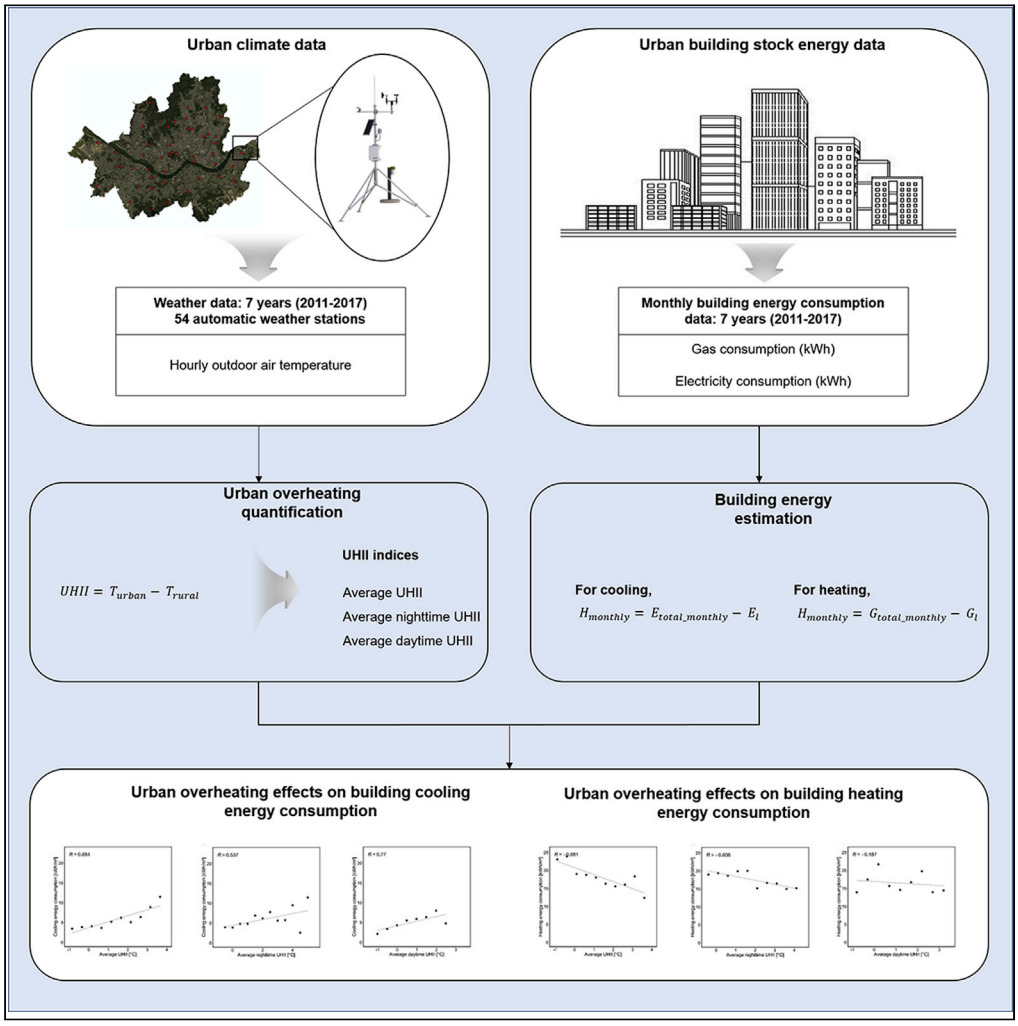

Mi Aye Su, Jack Ngarambe, Mat Santamouris, Geun Young Yun

gyyun@khu.ac.kr

Highlights

Real energy data used to study the effect of local climates on building energy use.

Cooling energy rises between 0.17 and 1.84 kWh/m^2 due to 0.5 K urban overheating.

Heating energy drops between 0.06 and 1.19 kWh/m^2 due to 0.5 K urban overheating.

Urban overheating effects are more exacerbated during the cooling period.

Su et al., iScience *24*, 102495
May 21, 2021
https://doi.org/10.1016/j.isci.2021.102495

iScience

CellPress
OPEN ACCESS

Article

Empirical evidence on the impact of urban overheating on building cooling and heating energy consumption

Mi Aye Su,[1] Jack Ngarambe,[1] Mat Santamouris,[1,2] and Geun Young Yun[1,3,*]

SUMMARY

A primary contributor to urban overheating is the urban heat island (UHI) formed due to increased urbanization. The adverse effects of UHI on building energy use are substantial and well documented. However, such effects are typically demonstrated through numerical simulations which are susceptible to modeling uncertainties and lack of validation resulting in a pressing research gap. Here, for the first time, we conduct a large-scale assessment to demonstrate the devastating impact of UHI on building energy consumption using real building energy use data. We find empirical evidence correlating UHI with building energy use; changes in average UHI intensity of 0.5 K correspond to an increase in monthly cooling energy consumption in a range of 0.17 kWh/m^2–1.84 kWh/m^2. The study validates theoretical evidence on the impact of UHI on building energy and proposes a highly innovative methodology to assess the impact of overheating on the energy balance of cities.

INTRODUCTION

Urban overheating is an essential topic in urban climatic studies owing to its impediment on the various aspects of the urban existence/ecosystem. The most important contributor to urban overheating is, arguably, the urban heat island (UHI) resulting from various physioclimatic processes that modulate the urban thermal structure. A distinctive outcome of UHI is often urban environments that are relatively hotter than their natural surroundings reaching a peak difference of up to 10 K (Santamouris, 2020).

The primary drivers that lead to UHI formation are well documented in the literature and are mainly due to (I) changes in the energy surface budget as a result of increased heat storage capacities by heavy infrastructural materials found in urban areas, (II) reduction in horizontal convective cooling mechanisms (i.e., winds) as they are blocked by large buildings found in urban areas, and (III) increased anthropogenic heat release owing to high population densities often found in urban areas (Fitria et al., 2019; Li et al., 2020; Manoli et al., 2019). A combination of these factors has an apparent and substantial effect on urban climates which hinders progress toward sustainable, livable cities.

While the repercussions of urban overheating are multifaceted and naturally diverse, they can be subtly grouped into three broad categories: (I) direct impact on urban dwellers in terms of exerted thermal stress, especially in the summertime or periods of extreme heat events and which results in increased heat-related thermal discomfort, mortalities, and morbidities (Founda and Santamouris, 2017; He et al., 2021; Ngarambe et al., 2020), (II) heightened urban air pollution levels resulting from synergistic interactions between UHI-related elevated temperatures and atmospheric pollutants often fueled by complex photochemical processes (Cao et al., 2016; Ngarambe et al., 2021; Ulpiani, 2021), and (III) a serious impact on the energy demand of cities; they increase the cooling load and partially decrease the heating load (Li et al., 2019; Santamouris, 2014).

Research on the influence of urban overheating on building energy, in particular, has picked up pace fundamentally because it constitutes substantial and extensive implications on global energy consumption and subsequently increased carbon footprints that may exacerbate long-term effects of climate change. Numerous studies were conducted to investigate the energy impact of UHI on the energy budget of cities and are well summarized in Santamouris (2014) and Li et al. (2019). These studies reveal a serious impact of

[1]Department of Architectural Engineering, Kyung Hee University, 1732, Deogyeong-daero, Giheung-gu, Yongin-si, Gyeonggi-do 17104, Republic of Korea

[2]Facaulty of Built Environment, University of New South Wales, Sydney, Australia

[3]Lead contact

*Correspondence: gyyun@khu.ac.kr

https://doi.org/10.1016/j.isci.2021.102495

UHI on city-wide energy consumption. In particular, it is found that, on average, UHI-related urban overheating causes an additional peak electricity demand close to 21 W per unit degree change in temperature per person and an additional cooling energy penalty close to 0.7 KWh per square meter of a city per unit degree temperature change (Santamouris et al., 2015).

While the direct effect of UHI-related urban overheating is substantial and evident in the existing literature, the typical approach of demonstrating such effects has mostly been theoretical in nature and all existing studies, entirely or partially, employ numerous simulation methodologies which are characterized by non-homogeneity and lack of validation making the existing conclusions on the impact of UHI on energy demand substantially different. Consequently, there is a severe uncertainty and a considerable research gap regarding the real impact of regional climate change on the energy balance of cities. Moreover, given that overheating is expected to seriously increase in the near future due to global climate change and increased urbanization, there is an urgent need to assess the real impact of urban overheating on the energy balance using large-scale, city-wide energy and long-term climatic data.

Here, for the first time, we present a longitudinal large-scale assessment engrossing seven years of and temperature observations from a dense network of observatories (i.e., 54 automatic weather stations) and real energy data from all buildings within a 200 m radius of each weather station to demonstrate the real effect of regional climates on city-wide building energy consumption.

We find empirical evidence demonstrating the effect of UHI on building energy use. For instance, we find that rises in average UHI intensity (UHII) of 0.5 K correspond to an increase in monthly cooling energy consumption in a range of 0.89 kWh/m^2–1.84 kWh/m^2 and a decrease in monthly heating energy consumption in a range of 0.3 kWh/m^2–1.19 kWh/m^2 depending mainly on the size of the residential neighborhood facility. Moreover, average nocturnal UHII better correlates with monthly building energy consumption than average daytime UHII. For example, changes of 0.5 K in nighttime UHII correspond to monthly cooling energy consumption increases ranging between 0.69 kWh/m^2 and 1.51 kWh/m^2. In contrast, the same UHII changes during the daytime correspond to monthly cooling energy increases ranging between 0.17 kWh/m^2 and 0.38 kWh/m^2.

The present study is the first to assess the impact of urban overheating on the urban energy balance using large-scale and city-wide energy and climatic data and proposes a robust innovative methodology to assess the impact of overheating on the energy balance of cities and can be used as a standard for future assessments.

RESULTS

Empirical evidence of UHI on building cooling energy use

We found that UHII had positive correlations with cooling energy consumption, indicating that a rise in UHII resulted in increased cooling energy consumption. We considered class 1 residential neighborhood facilities and class 2 residential neighborhood facilities (please see the STAR Methods section for the detailed information on the types of buildings considered). Among the analyzed three UHII indicators (i.e. average UHII, average daytime UHII, and average nighttime UHII), we observed that the average UHII had the highest impact on building cooling energy consumption in both class 1 and class 2 residential neighborhood facilities.

Our analysis indicated a high coefficient of correlation (R) between average UHII and building cooling energy consumption for class 1 residential neighborhood facilities (R = 0.545) and class 2 residential neighborhood facilities (R = 0.884). For instance, average cooling energy consumption for the low-level UHII bin was 5.79 $\pm$ 0.7 kWh/m^2 (mean $\pm$ 1 standard error mean) while that for the high-level UHII bin was 22.32 $\pm$ 20.47 kWh/m^2 for class 1 residential neighborhood facilities (see Figure 1A). Similarly, average cooling energy consumption for the low-level UHII bin was 3.45 $\pm$ 0.55 kWh/m^2 while that for the high-level UHII bin was 11.47 $\pm$ 8.75 kWh/m^2 for class 2 residential neighborhood facilities (see Figure 1B). The variances in mean cooling energy consumption among average UHII groups were statistically significant ($p < 0.005$) (see Table 1).

Furthermore, the coefficients of correlation between average nighttime UHII and building cooling energy consumption were 0.505 and 0.537 for class 1 and class 2 residential neighborhood facilities, respectively.

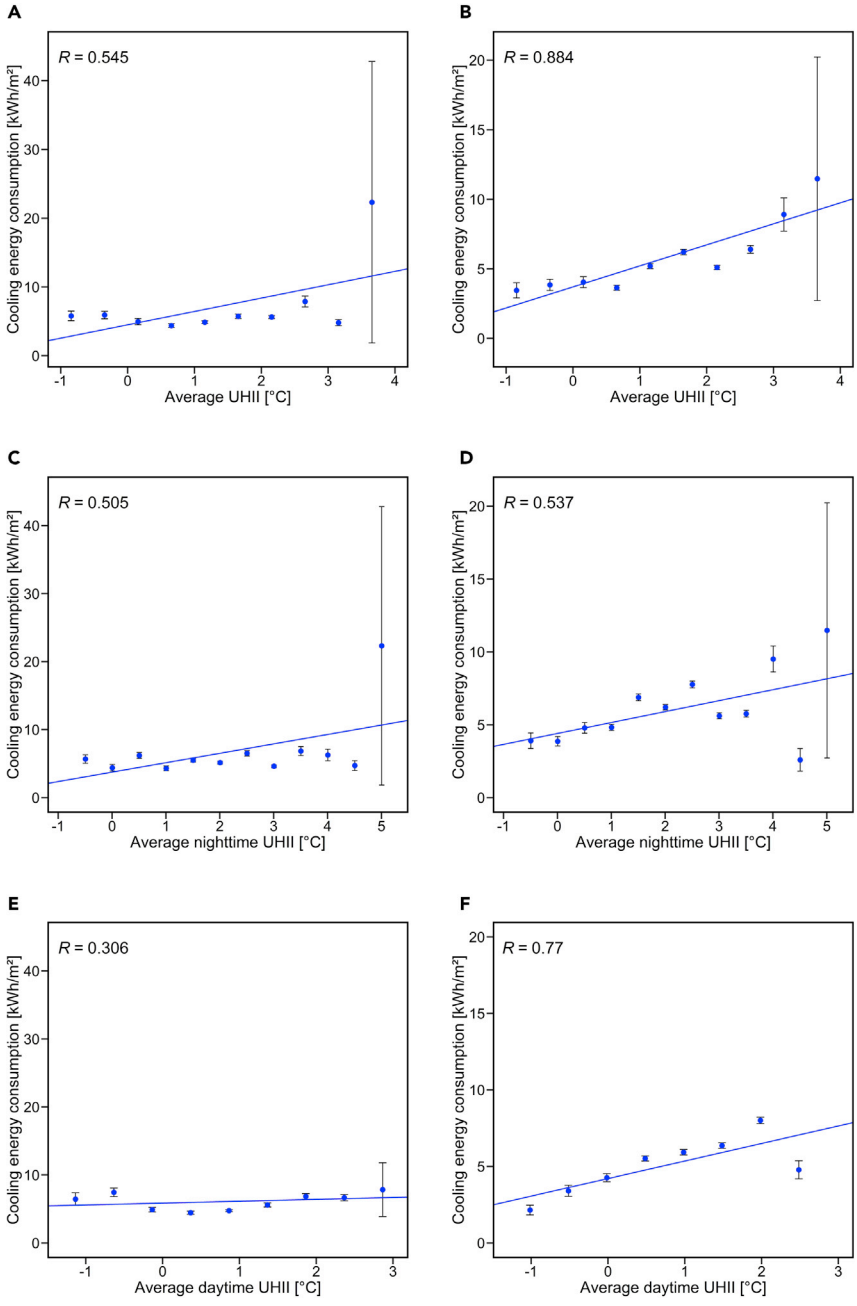

Figure 1. Relationships between different UHII indicators and building cooling energy consumption

(A–F) Relationships between average UHII and cooling energy consumption for class 1 residential neighborhood facilities (A) and for class 2 residential neighborhood facilities (B), relationships between average nighttime UHII and cooling energy consumption for class 1 residential neighborhood facilities (C) and for class 2 residential neighborhood facilities (D), and relationships between average daytime UHII and cooling energy consumption for class 1 residential neighborhood facilities (E) and for class 2 residential neighborhood facilities (F). Error bars indicate ± 1 standard error mean.

Also, average cooling energy consumption for the low-level UHII bin was 5.67 ± 0.63 kWh/m^2 while that for the high-level UHII bin was 22.32 ± 20.47 kWh/m^2 for class 1 residential neighborhood facilities (see Figure 1C). For class 2 residential neighborhood facilities, average cooling energy consumption for the low-level UHII bin was 3.90 ± 0.53 kWh/m^2 while that for the high-level UHII bin was 11.47 ± 8.75 kWh/m^2 (see Figure 1D). These differences in mean cooling energy consumption across the nighttime UHII groups

Table 1. Kruskal-Wallis test for building energy versus UHII

No	Building type	UHII indicators	Cooling season			Heating season		
			df	X^2	p	df	X^2	p
1	Class 1 residential neighborhood facilities	Average	9	86.11	<0.005	9	231.4	<0.005
		Average nighttime	11	156.5	<0.005	10	304.9	<0.005
		Average daytime	8	135.1	<0.005	9	212.3	<0.005
2	Class 2 residential neighborhood facilities	Average	9	195.1	<0.005	9	374.2	<0.005
		Average nighttime	11	476.4	<0.005	9	443.0	<0.005
		Average daytime	7	232.6	<0.005	8	270.1	<0.005

were statistically significant ($p < 0.005$) (see Table 1). We also observed positive correlations between average daytime UHII and building cooling energy consumption (see Figures 1E and 1F). Average cooling energy consumption for class 1 residential neighborhood facilities for the low-level UHII bin was 6.44 $\pm$ 0.93 kWh/m^2 while that for the high-level UHII bin was 7.84 $\pm$ 3.95 kWh/m^2 (see Figure 1E). For class 2 residential neighborhood facilities, average cooling energy consumption for the low-level UHII bin was 2.15 $\pm$ 0.32 kWh/m^2 while that for the high-level UHII bin was 4.78 $\pm$ 0.59 kWh/m^2 (see Figure 1F). The variances in mean cooling energy consumption among average daytime UHII groups were statistically significant ($p < 0.005$) (see Table 1). The observed deviations in the general trend seen in Figure 1 are possibly due to the different space use by the considered buildings which likely increase the variance in the data.

Empirical evidence of UHI on building heating energy use

Our results show a significant relationship between UHII and heating energy consumption of the buildings. We found that heating energy consumption decreased with increasing UHII. Also, average nighttime UHII had the highest impact on the heating energy consumption of class 1 residential neighborhood facilities while average UHII had the highest influence on the heating energy consumption of class 2 residential neighborhood facilities.

Based on the analysis, we found a high coefficient of correlation ($R = 0.809$) between average nighttime UHII and building heating energy consumption for class 1 residential neighborhood facilities. It was also observed that average heating energy consumption for the low-level UHII bin was 13.71 $\pm$ 1.63 kWh/m^2 while that for the high-level UHII bin was 6.17 $\pm$ 2.45 kWh/m^2 (see Figure 2A) suggesting reduced heating energy requirements when UHII is high. Similar results were obtained for class 2 residential neighborhood facilities ($R = 0.806$); average heating energy consumption for the low-level UHII bin was 18.99 $\pm$ 3.34 kWh/m^2 while that for the high-level UHII bin was 15.22 $\pm$ 0.97 kWh/m^2 (see Figure 2B). The variances in mean heating energy consumption among average nighttime UHII groups were statistically significant ($p < 0.005$) (see Table 1).

Furthermore, negative correlations were observed between average UHII and building heating energy consumption (see Figures 2C and 2D). For instance, average heating energy consumption for class 1 residential neighborhood facilities for the low-level UHII bin was 13.29 $\pm$ 1.43 kWh/m^2 while that for the high-level UHII bin was 10.62 $\pm$ 0.82 kWh/m^2 (see Figure 2C). For class 2 residential neighborhood facilities, average heating energy consumption for the low-level UHII bin was 23.08 $\pm$ 3.87 kWh/m^2 while that for the high-level UHII bin was 12.37 $\pm$ 1.52 kWh/m^2 (see Figure 2D). The variances in mean heating energy consumption among average UHII groups were statistically significant ($p < 0.005$) (see Table 1).

Similarly, negative correlations were observed between average daytime UHII and building heating energy consumption (see Figures 2E and 2F). As an example, for class 1 residential neighborhood facilities, average heating energy consumption for the low-level UHII bin was 15.41 $\pm$ 1.29 kWh/m^2 while that for the high-level UHII bin was 13.55 $\pm$ 1.13 kWh/m^2. For class 2 residential neighborhood facilities, average heating energy consumption for the low-level UHII bin was 17.45 $\pm$ 1.00 kWh/m^2 while that for the high-level UHII bin was 14.14 $\pm$ 1.96 kWh/m^2. Moreover, the variances in mean heating energy consumption among average daytime UHII groups were statistically significant ($p < 0.005$) (see Table 1). The observed deviations in the general trend seen in Figure 2 are possibly due to the different space use by the considered buildings which likely increase the variance in the data.

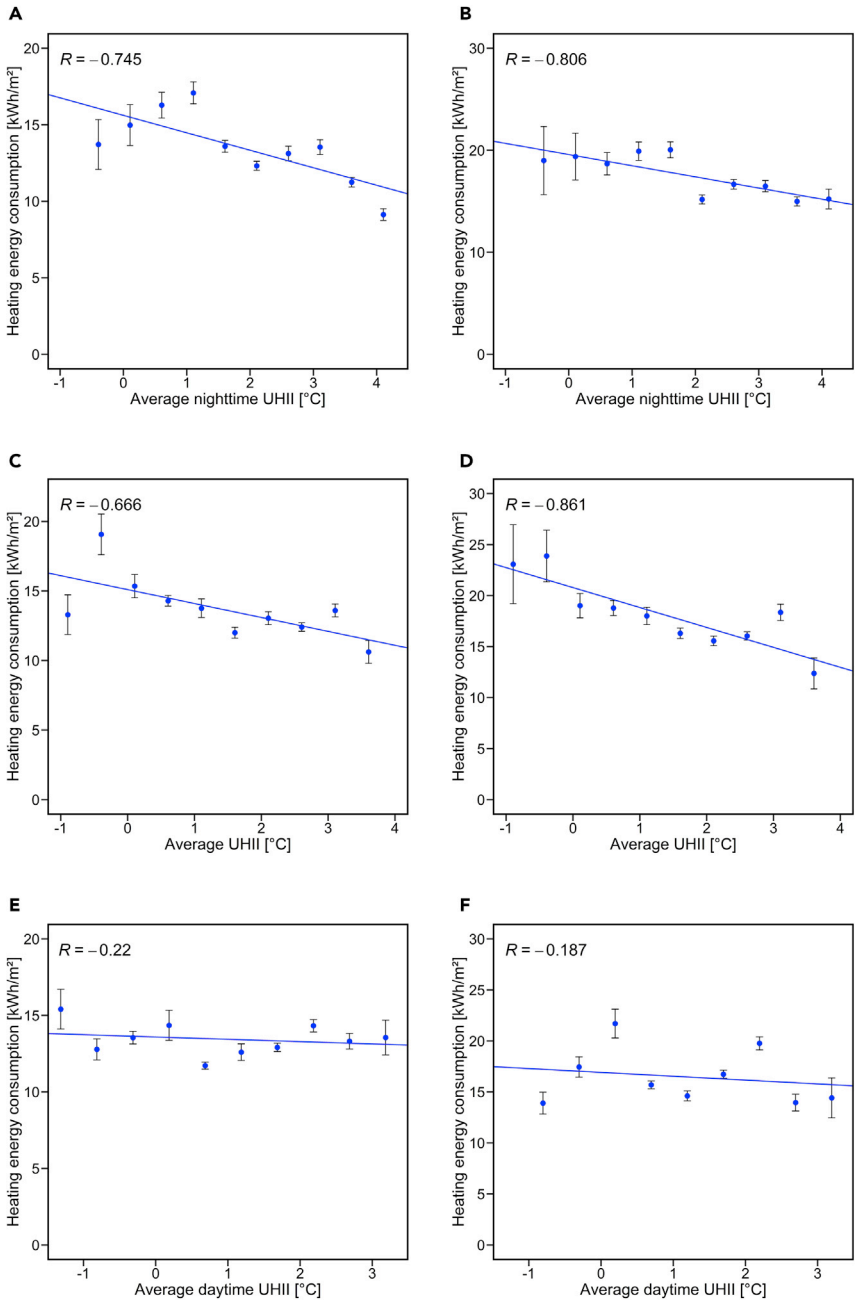

Figure 2. Relationships between different UHII indicators and building heating energy consumption

(A–F) Relationships between average nighttime UHII and heating energy consumption for class 1 residential neighborhood facilities (A) and for class 2 residential neighborhood facilities (B), relationships between average UHII and heating energy consumption for class 1 residential neighborhood facilities (C) and for class 2 residential neighborhood facilities (D), and relationships between average daytime UHII and heating energy consumption for class 1 residential neighborhood facilities (E) and for class 2 residential neighborhood facilities (F). Error bars indicate ± 1 standard error mean.

Influence of outdoor temperature on building energy use

As expected, our analysis confirms the positive correlations between outdoor air temperature and cooling energy (see Figures 3A and 3B). For instance, average cooling energy consumption for class 1 residential neighborhood facilities for the low-level average temperature bin was 4.51 ± 0.33 kWh/m^2 while that for

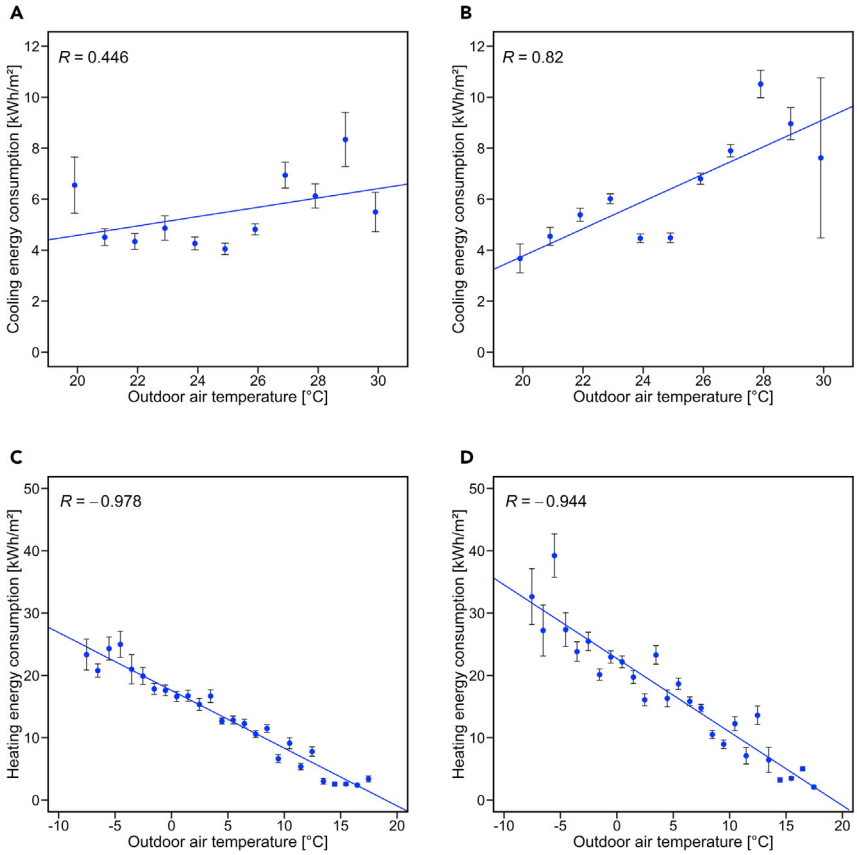

Figure 3. Relationships between outdoor air temperature and building cooling and heating energy consumption

(A–D) Class 1 residential neighborhood facilities cooling season (A), class 2 residential neighborhood facilities cooling season (B), class 1 residential neighborhood facilities heating season (C), and class 2 residential neighborhood facilities heating season (D). Error bars indicate ± 1 standard error mean.

the high-level average temperature bin was 5.49 ± 0.77 kWh/m^2. For class 2 residential neighborhood facilities, average cooling energy consumption for the low-level average temperature bin was 3.67 ± 0.57 kWh/m^2 while that for the high-level average temperature bin was 7.62 ± 3.14 kWh/m^2; these differences were statistically significant (see Table 2).

It was also observed that an increase in outdoor air temperature resulted in decreased heating energy consumption (see Figures 3C and 3D). For example, for class 1 residential neighborhood facilities, average heating energy consumption for the low-level average temperature bin was 23.33 ± 2.48 kWh/m^2 while that for the high-level average temperature bin was 3.38 ± 0.47 kWh/m^2. For class 2 residential neighborhood facilities, average heating energy consumption for the low-level average temperature bin was 32.63 ± 4.49 kWh/m^2 while that for the high-level average temperature bin was 2.09 ± 0.24 kWh/m^2; these differences were also statistically significant (see Table 2).

Energy use differences between rural and urban buildings

Our results show that the cooling degree days (CDDs) in the rural reference site (see the STAR Methods section for details on the determination of the rural reference site) were lower than those in the urban station (see Figure 4A). In contrast, the heating degree days (HDDs) were higher in the rural station than in the urban station (see Figure 4B). These results insinuate higher cooling energy consumption but lower heating energy consumption in urban areas compared to rural areas likely because of the UHI-related overheating.

This result is further reinforced by the particular correlations found between CDDs, HDDs, and building energy consumption. For example, our data show that cooling energy consumption increased with increasing

Table 2. Kruskal-Wallis test for building energy versus outdoor air temperature

		Cooling season			Heating season		
No	Types of building	df	X^2	P	df	X^2	p
1	Class 1 residential neighborhood facilities	10	514.37	<0.005	25	7506.34	<0.005
2	Class 2 residential neighborhood facilities	10	1136.54	<0.005	25	6301.62	<0.005

CDDs. For class 1 residential neighborhood facilities, average cooling energy consumption for the low-level CDD bin was 4.38 $\pm$ 0.15 kWh/m^2 while that for the high-level CDD bin was 14.35 $\pm$ 2.72 kWh/m^2 (see Figure 4C). For class 2 residential neighborhood facilities, average cooling energy consumption for the low-level CDD bin was 5.11 $\pm$ 0.12 kWh/m^2 while that for the high-level CDD bin was 12.22 $\pm$ 1.59 kWh/m^2 (see Figure 4D). The variances in mean cooling energy consumption among CDD groups were statistically significant according to the Kruskal-Wallis test: X^2 (13) = 804.384, $P < 0.005$ for class 1 residential neighborhood facilities and X^2 (13) = 1183.557, $P < 0.005$ for class 2 residential neighborhood facilities. Similarly, it was observed that heating energy consumption increased with increasing HDDs for both class 1 residential neighborhood facilities (see Figure 4E) and class 2 residential neighborhood facilities (see Figure 4F). This relationship was also statistically significant according to the Kruskal-Wallis test: X^2 (18) = 6660.105, $P < 0.005$ and X^2 (13) = 4728.336, $P < 0.005$ for class 1 and class 2 residential neighborhood facilities, respectively.

DISCUSSION

One of the fundamental topics in building energy research relates to the minimization of building energy use through efficient, practical design methods or energy use regulatory schemes. In fact, theoretical studies, as well as field projects that employ zero-energy concepts, have increased over the years and will likely increase in the near future. A vital element of developing such efficient methods involves a full understanding of the many drivers likely to influence building energy consumption (Copiello and Gabrielli, 2017). A primary determinant of building energy consumption in urban areas is urban overheating resulting from the UHI phenomenon (defined in the introduction).

While the potential effects of UHI-related urban heating on building energy consumption are well understood theoretically (Li et al., 2019), it is challenging to quantify such effects for several reasons, but primarily because, while meteorological data through which UHI estimates can be computed are vastly available, building energy data are often not readily available and challenging to collect through field measurements, especially for a group/stock of buildings. Consequently, most existing studies that quantitatively explore the influence of UHI are broadly categorized into two types: (I) studies that rely on building simulation tools to model the effect of UHI on building energy or (II) studies that rely on monitored air temperature data and observed/simulated energy data from a limited number of buildings. The first type of studies (i.e., simulation based), while they provide practical means of assessing the effect of UHI on building energy consumption, is still susceptible to errors from the individual limitations of the modeler and the results often subjective rather than objective. The second set of studies (i.e., based on in situ temperature and observed building energy data) often employs temperature data collected over a short period and energy data collected from a limited number of buildings of the same function. A recent extensive review on the effects of UHI on building energy consumption identified twenty-four articles that explicitly discuss the quantitative impact of UHI on building energy; nine of identified studies employed simulation tools while the remainder use the short-term temperature data and energy data obtained from/simulated for single buildings of the same function (e.g., a single office building located in an urbanized area and a corresponding office reference building situated in a rural or suburban area) (Li et al., 2019). To overcome such shortcomings, this article demonstrates the influence of urban overheating through empirical observations of energy use profiles and large records of outdoor air temperature.

Our results show that both UHI and air temperature have a substantial and statistically significant effect on building energy consumption regardless of the building size. However, the nature of the said effect differs between UHI and ambient air temperature, particularly during the heating season. On the one hand, the low temperatures associated with cold seasons often increase heating energy requirements. On the other hand, the UHI-related increase in temperature during the cold season is likely to reduce heating energy

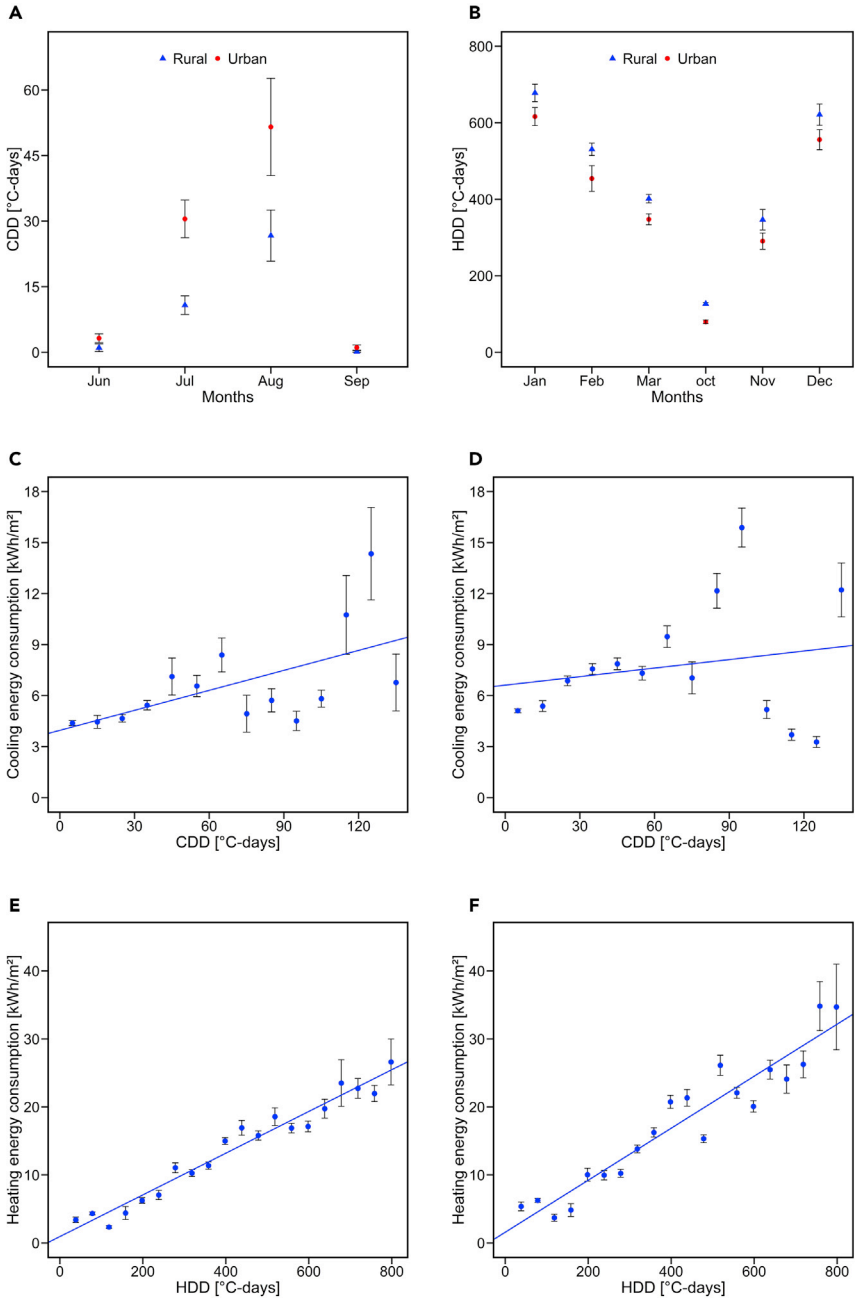

Figure 4. CDD differences in rural and urban stations

(A–F) (A), HDD differences in rural and urban stations (B), relationships between CDD and cooling energy consumption for class 1 residential neighborhood facilities (C) and for class 2 residential neighborhood facilities (D), and relationships between HDD and heating energy consumption for class 1 residential neighborhood facilities (E) and for class 2 residential neighborhood facilities (F). Error bars indicate ± 1 standard error mean.

requirements. For example, our results show that an increase of 0.5 K in monthly UHII is likely to result in a decrease in monthly heating energy in the range of 0.21 kWh/m^2 to 0.75 kWh/m^2 for class 1 residential neighborhood facilities and 0.06 kWh/m^2 to 1.19 kWh/m^2 for class 2 residential neighborhood facilities.

The corresponding effect of UHI on building energy consumption during the cooling season is rather direct; an increase in 0.5 K in monthly UHI is likely to increase monthly cooling energy in the range of

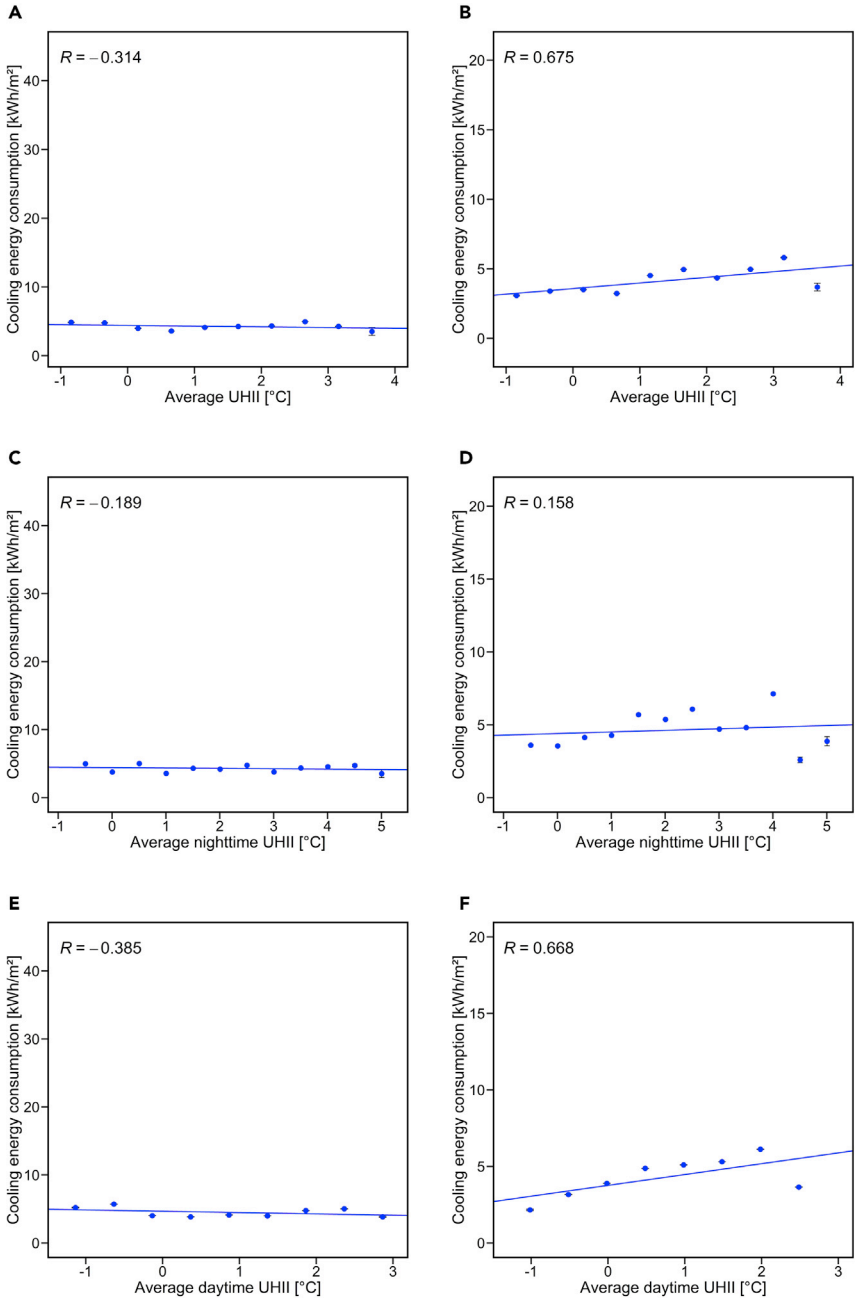

Figure 5. Relationships between different UHII indicators and building cooling energy consumption

(A–F) Relationships between average UHII and cooling energy consumption for class 1 residential neighborhood facilities (A) and for class 2 residential neighborhood facilities (B), relationships between average nighttime UHII and cooling energy consumption for class 1 residential neighborhood facilities (C) and for class 2 residential neighborhood facilities (D), and relationships between average daytime UHII and cooling energy consumption for class 1 residential neighborhood facilities (E) and for class 2 residential neighborhood facilities (F). Error bars indicate ± 1 standard error mean.

0.17 kWh/m^2 to 1.84 kWh/m^2 for class 1 residential neighborhood facilities and 0.38 kWh/m^2 to 0.89 kWh/m^2 for class 2 residential neighborhood facilities. Our results reiterate previous reports in major global cities such as Rome (Zinzi and Carnielo, 2017), Tokyo (Hirano and Fujita, 2012), Beijing (Cui et al., 2017), and London (Kolokotroni et al., 2007; Watkins et al., 2002). The possible reasons for the positive effect of UHI on heating energy requirements and its negative impact on cooling energy requirements are, theoretically,

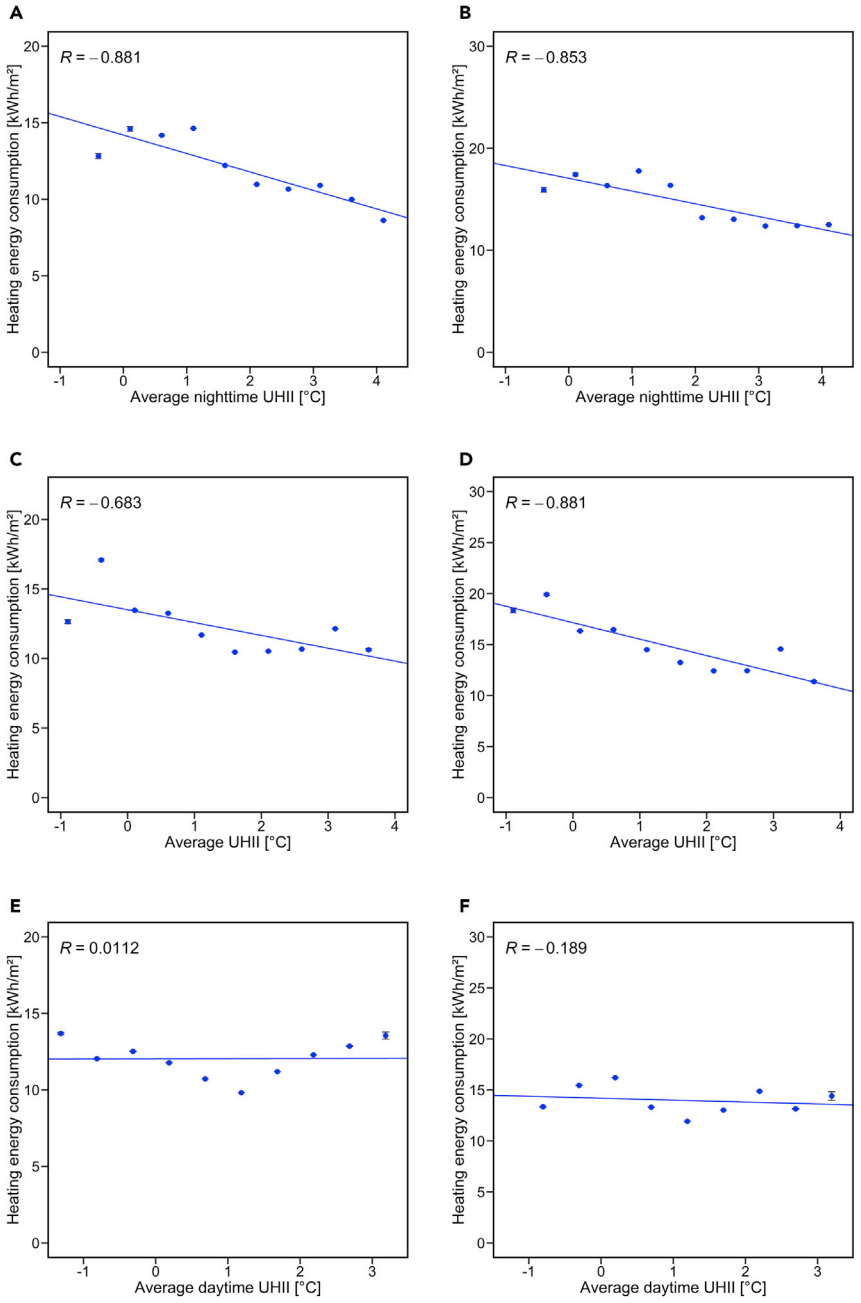

Figure 6. Relationships between different UHII indicators and building heating energy consumption

(A–F) Relationships between average nighttime UHII and heating energy consumption for class 1 residential neighborhood facilities (A) and for class 2 residential neighborhood facilities (B), relationships between average UHII and heating energy consumption for class 1 residential neighborhood facilities (C) and for class 2 residential neighborhood facilities (D), and relationships between average daytime UHII and heating energy consumption for class 1 residential neighborhood facilities (E) and for class 2 residential neighborhood facilities (F). Error bars indicate ± 1 standard error mean.

well explained in the literature and are, in a way, rooted in the fundamental definition of UHI itself (Oke, 1982). UHI is the increase in air temperature resulting from solar heat storage by low emissivity materials in the form of short-wave solar radiation. This stored insolation once re-emitted (i.e. in the form of long wave solar radiation) exacerbates the effects of typically high temperatures during the cooling season and reduces the heating needs during low-temperature periods (i.e., the heating season).

The results of the current research demonstrate, through empirical observations, the seriousness of urban overheating on building energy consumption and thus a critical step toward practical discussions with potential contributions on sustainable urban areas, salutogenic urban design practices, and the overall urban liveability agenda. For instance, given the seriousness of urban overheating established in this study, these discussions should be centered around encouraging the flow of capital investment to support various urban overheating techniques such green infrastructures, cool roofs, etc. or to support national building code amendments for purposes of minimizing heat accumulation and improving energy-efficient cooling on the urban level or individual building level. Moreover, such discussions should be prioritized toward energy-poor demographics who might be unable to cope with UHI-related heightened temperatures via active cooling methods.

It is also worth noting that there are certain deviations in the relationship between building energy and UHII (see Figures 1 and 2). Such deviations result from extreme values in the collected energy data (i.e., outliers). A similar analysis without outliers is included here (see Figures 5 and 6). However, we chose to focus on the analysis with outliers mainly due to the nature of the analyzed buildings. The two classes of buildings include facilities such as retail stores, restaurants, bakeries, religious facilities, local government centers (i.e., fire stations, post offices, etc.) whose energy use may vary widely despite being the same size. We were thus reluctant to identify very large values or very low values as outliers as they may as well not have been outliers. To account for this dynamism to an extent, we opted for a non-parametric procedure to quantify the potential mean differences among the different UHII bins. Nevertheless, we feel that normalizing our analysis, for instance, by considering only those buildings of similar space use (e.g., only fire stations or only post offices), would have better illustrated the influence of UHII on building energy consumption.

Limitations of the study

One major limitation of the current study concerns the extrapolation of the obtained results to other localities. Further studies that develop white-box models relating building energy consumption to the local climate and other relevant factors are warranted. For instance, a complied data set of building energy use that reflects the potential effects of local overheating (e.g., from buildings in an urban environment) could be divided into two distinct portions and one used for the development of the said physics model and the remaining portion as a validation set.

Another apparent limitation of the current study concerns the space use of the considered facilities. While the facilities are all multi-living neighborhood facilities (e.g., retails shops, churches) categorized on the basis of surface area to form two categories, class 1 residential neighborhood facilities (<1000 m^2) and class 2 residential neighborhood facilities (<500 m^2), there is likely still substantial differences in how the individual spaces are used regardless of their sizes. One way to overcome this limitation, which perhaps warrants exploration, would entail the consideration of only one type of building based on function (i.e., assess the impact of overheating on building energy consumption by retail stores).

Furthermore, while the segregation method used to determine the heating and cooling energy has been widely employed (Ahn et al., 2019; Robison, 1992; Kwag et al., 2020), the obtained results are still a crude estimate of the real heating and cooling energy. Future research is encouraged to employ improved estimation methods in determining heating and cooling energy use.

STAR★METHODS

Detailed methods are provided in the online version of this paper and include the following:

- KEY RESOURCES TABLE
- RESOURCE AVAILABILITY
  - Lead contact
  - Materials availability
  - Data and code availability
- METHODS DETAILS
  - Study site and in situ observations
  - Calculating urban heat island intensity
  - Building information and functions

- Cooling and heating energy consumption data
- Computing CDDs and HDDs
- QUANTIFICATION AND STATISTICAL ANALYSIS

SUPPLEMENTAL INFORMATION

Supplemental information can be found online at https://doi.org/10.1016/j.isci.2021.102495.

ACKNOWLEDGMENTS

This work was supported by the National Research Foundation of Korea (NRF) grant funded by the Korean government (MSIT) (No. 2020R1A2C1099611).

AUTHOR CONTRIBUTIONS

Conceptualization, G.Y.Y. and M.S.; methodology, G.Y.Y. and M.S.; supervision, G.Y.Y.; formal analysis, G.Y.Y., M.S., J.N., and M.A.S.; data curation, M.A.S.; writing – original draft, M.A.S. and J.N.; writing – review & editing, G.Y.Y. and M.S.; visualization, M.A.S.; funding fcquisition, G.Y.Y.

DECLARATION OF INTERESTS

The authors declare no competing interests.

Received: February 17, 2021
Revised: April 5, 2021
Accepted: April 26, 2021
Published: May 21, 2021

REFERENCES

Ahn, K., Shin, H., and Park, C. (2019). Energy analysis of 4625 office buildings in South Korea. Energies *12*, 1114. https://doi.org/10.3390/en12061114.

ASHRAE (2001). 2001 ASHRAE Handbook: Fundamentals (American Society of Heating, Refrigerating and Air-Conditioning Engineers), p. 544.

Cao, C., Lee, X., Liu, S., Schultz, N., Xiao, W., Zhang, M., and Zhao, L. (2016). Urban heat islands in China enhanced by haze pollution. Nat. Commun. *7*, 12509. https://doi.org/10.1038/ncomms12509.

Choi, Y. (2005). Temporal and spatial variability of heating and cooling degree days in South Korea, 1973-2002. J. Korean Geogr. Soc. *40*, 584–594.

Cohen, R., Standeven, M., Bordass, B., and Leaman, A. (2001). Assessing building performance in use 1: the Probe process. Building Res. Inf. *29*, 85–102. https://doi.org/10.1080/09613210010008018.

Copiello, S., and Gabrielli, L. (2017). Analysis of building energy consumption through panel data: the role played by the economic drivers. Energy Buildings *145*, 130–143. https://doi.org/10.1016/j.enbuild.2017.03.053.

Cui, Y., Yan, D., Hong, T., and Ma, J. (2017). Temporal and spatial characteristics of the urban heat island in Beijing and the impact on building design and energy performance. Energy *130*, 286–297. https://doi.org/10.1016/j.energy.2017.04.053.

Field, J., Soper, J., Jones, P., Bordass, W., and Grigg, P. (1997). Energy performance of occupied non-domestic buildings: assessment by analysing end-use energy consumptions. Building Serv. Eng. Res. Technol. *18*, 39–46. https://doi.org/10.1177/014362449701800106.

Fitria, R., Kim, D., Baik, J., and Choi, M. (2019). Impact of biophysical mechanisms on urban heat island associated with climate variation and urban morphology. Sci. Rep. *9*, 19503. https://doi.org/10.1038/s41598-019-55847-8.

Founda, D., and Santamouris, M. (2017). Synergies between urban heat island and heat waves in athens (Greece), during an extremely hot summer (2012). Sci. Rep. *7*, 10973. https://doi.org/10.1038/s41598-017-11407-6.

Gastwirth, J.L., Gel, Y.R., and Miao, W. (2009). The impact of Levene's test of equality of variances on statistical theory and practice. Stat. Sci. *24*, 343–360.

Guattari, C., Evangelisti, L., and Balaras, C.A. (2018). On the assessment of urban heat island phenomenon and its effects on building energy performance: a case study of Rome (Italy). Energy Buildings *158*, 605–615. https://doi.org/10.1016/j.enbuild.2017.10.050.

He, B.-J., Wang, J., Liu, H., and Ulpiani, G. (2021). Localized synergies between heat waves and urban heat islands: implications on human thermal comfort and urban heat management. Environ. Res. *193*, 110584. https://doi.org/10.1016/j.envres.2020.110584.

Hirano, Y., and Fujita, T. (2012). Evaluation of the impact of the urban heat island on residential and commercial energy consumption in Tokyo. Energy *37*, 371–383. https://doi.org/10.1016/j.energy.2011.11.018.

Kim, Y.H., and Baik, J.J. (2002). Maximum urban heat island intensity in Seoul. J. Appl. Meteorol. *41*, 651–659. https://doi.org/10.1016/j.solener.2006.06.005.

Kolokotroni, M., Zhang, Y., and Watkins, R. (2007). The London Heat Island and building cooling design. Solar Energy *81*, 102–110. https://doi.org/10.1016/j.solener.2006.06.005.

Korea Information Society Agency n.d, Public Data Portal, Korea Information Society Agency, viewed 2 February 2020, <https://www.data.go.kr/index.do>

Korea Meteorological Administration n.d, Weather Data Opening Portal, Korea Meteorological Administration, viewed 1 October 2019, https://data.kma.go.kr/cmmn/main.do

Kwag, B.C., Han, S., Kim, G.T., Kim, B., and Kim, J.Y. (2020). Analysis of the effects of strengthening building energy policy on multifamily residential buildings in South Korea. Sustainability *12*, 3566. https://doi.org/10.3390/su12093566.

Lee, K., Baek, H.-J., and Cho, C. (2014). The estimation of base temperature for heating and cooling degree-days for South Korea. J. Appl. Meteorol. Climatol. *53*, 300–309. https://doi.org/10.1175/JAMC-D-13-0220.1.

Lee, S.-H., Song, C.-K., Baik, J.-J., and Park, S.-U. (2009). Estimation of anthropogenic heat emission in the Gyeong-In region of Korea. Theor. Appl. Climatol. *96*, 291–303. https://doi.org/10.1007/s00704-008-0040-6.

Lee, Y.Y., Kim, J.T., and Yun, G.Y. (2016). The neural network predictive model for heat island intensity in Seoul. Energy Buildings *110*, 353–361. https://doi.org/10.1016/j.enbuild.2015.11.013.

Li, C., Zhou, J., Cao, Y., Zhong, J., Liu, Y., Kang, C., and Tan, Y. (2014). Interaction between urban microclimate and electric air-conditioning energy consumption during high temperature season. Appl. Energy *117*, 149–156. https://doi.org/10.1016/j.apenergy.2013.11.057.

Li, X., Zhou, Y., Yu, S., Jia, G., Li, H., and Li, W. (2019). Urban heat island impacts on building energy consumption: a review of approaches and findings. Energy *174*, 407–419. https://doi.org/10.1016/j.energy.2019.02.183.

Li, Y., Schubert, S., Kropp, J.P., and Rybski, D. (2020). On the influence of density and morphology on the Urban Heat Island intensity. Nat. Commun. *11*, 2647. https://doi.org/10.1038/s41467-020-16461-9.

Manoli, G., Fatichi, S., Schläpfer, M., Yu, K., Crowther, T.W., Meili, N., Burlando, P., Katul, G.G., and Bou-Zeid, E. (2019). Magnitude of urban heat islands largely explained by climate and population. Nature *573*, 55–60. https://doi.org/10.1038/s41586-019-1512-9.

Ministry of Government Legislation (1997). National Law Information Center (Ministry of Government Legislation). https://www.law.go.kr.

Ministry of Land, Infrastructure and Transport n.d. *Korea National Spatial Data Infrastructure Portal*, Ministry of Land, Infrastructure and Transport, viewed 1 October 2019, http://openapi.nsdi.go.kr/nsdi/eios/S erviceDetail.do

Ngarambe, J., Joen, S.J., Han, C.-H., and Yun, G.Y. (2021). Exploring the relationship between particulate matter, CO, SO2, NO2, O3 and urban heat island in Seoul, Korea. J. Hazard. Mater. *403*, 123615. https://doi.org/10.1016/j.jhazmat.2020.123615.

Ngarambe, J., Nganyiyimana, J., Kim, I., Santamouris, M., and Yun, G.Y. (2020). Synergies between urban heat island and heat waves in Seoul: the role of wind speed and land use characteristics. PLoS One *15*, e0243571. https://doi.org/10.1371/journal.pone.0243571.

Oh, J.W., Ngarambe, J., Duhirwe, P.N., Yun, G.Y., and Santamouris, M. (2020). Using deep-learning to forecast the magnitude and characteristics of urban heat island in Seoul Korea. Sci. Rep. *10*, 3559. https://doi.org/10.1038/s41598-020-60632-z.

Oke, T.R. (2004). Initial Guidance to Obtain Representative Meteorological Observations at Urban Sites.

Oke, T.R. (1982). The energetic basis of the urban heat island. Q. J. R. Meteorol. Soc. *108*, 1–24. https://doi.org/10.1002/qj.49710845502.

Robison, D. (1992). Pacific power: the use of short-term measurements to decompose commercial billing data into primary end uses. In ACEEE 1992 Summer Study on Energy Efficiency in Buildings, *vol. 3*ACEEE 1992 Summer Study on Energy Efficiency in Buildings (ACEEE), pp. 239–249.

Runnalls, K.E., and Oke, T.R. (2006). A technique to detect microclimatic inhomogeneities in historical records of screen-level air temperature. J. Clim. *19*, 959–978. https://doi.org/10.1175/JCLI3663.1.

Santamouris, M. (2014). On the energy impact of urban heat island and global warming on buildings. Energy Buildings *82*, 100–113. https://doi.org/10.1016/j.enbuild.2014.07.022.

Santamouris, M. (2020). Recent progress on urban overheating and heat island research. Integrated assessment of the energy, environmental, vulnerability and health impact. Synergies with the global climate change. Energy Buildings *207*, 109482. https://doi.org/10.1016/j.enbuild.2019.109482.

Santamouris, M., Cartalis, C., Synnefa, A., and Kolokotsa, D. (2015). On the impact of urban heat island and global warming on the power demand and electricity consumption of buildings—a review. Energy Buildings *98*, 119–124. https://doi.org/10.1016/j.enbuild.2014.09.052.

Stewart, I.D., and Oke, T.R. (2010). Thermal differentiation of local climate zones using temperature observations from urban and rural field sites. In Ninth Symposium on Urban Environment, pp. 2–6.

Time and date AS (1995). Sunrise, Sunset and Daylength (Time and date AS). https://www.timeanddate.com/sun/south-korea/seoul.

Ulpiani, G. (2021). On the linkage between urban heat island and urban pollution island: three-decade literature review towards a conceptual framework. Sci. Total Environ. *751*, 141727. https://doi.org/10.1016/j.scitotenv.2020.141727.

Wang, S., Yan, C., and Xiao, F. (2012). Quantitative energy performance assessment methods for existing buildings. Energy Buildings *55*, 873–888. https://doi.org/10.1016/j.enbuild.2012.08.037.

Watkins, R., Palmer, J., Kolokotroni, M., and Littlefair, P. (2002). The balance of the annual heating and cooling demand within the London urban heat island. Building Serv. Eng. Res. Technol. *23*, 207–213. https://doi.org/10.1191/0143624402bt043oa.

Zinzi, M., and Carnielo, E. (2017). Impact of urban temperatures on energy performance and thermal comfort in residential buildings. Energy Buildings *157*, 20–29. https://doi.org/10.1016/j.enbuild.2017.05.021.

STAR★METHODS

KEY RESOURCES TABLE

REAGENT or RESOURCE	SOURCE	IDENTIFIER
Other		
Urban overheating (urban heat island intensity)	Korea Meteorological Administration https://data.kma.go.kr/cmmn/main.do	N/A
Ambient air temperature	Korea Meteorological Administration https://data.kma.go.kr/cmmn/main.do	N/A
Building energy consumption	Korea Information Society Agency https://www.data.go.kr/index.do	N/A

RESOURCE AVAILABILITY

Lead contact

Requests for further information and resources should be directed to the lead contact, Geun Young Yun (gyyun@khu.ac.kr).

Materials availability

This study did not generate new materials.

Data and code availability

The data sets generated and analyzed during the current study are available from the corresponding author on reasonable request and with permission from the Korea Meteorological Administration and Seoul Metropolitan Government.

METHODS DETAILS

Study site and in situ observations

The studied set of buildings was located in Seoul, South Korea. Seoul (Latitude 37° 1′ N, 126° 58′ E) is the capital city of South Korea and covers a surface area of approximately 605.25 km^2. It is one of the most populated cities in the world (Lee et al., 2009), with more than 9.7 million inhabitants. It is located in the northwestern part of the country and has a humid subtropical climate influenced by the monsoons. As a result of rapid development, Seoul has seen rapid urbanization that has resulted in drastic land-use changes. Due to said changes in land use, Seoul experiences high UHI intensities which is often higher than those in other Korean cities as evidenced by numerous scientific studies (Kim and Baik, 2002; Hirano and Fujita, 2012; Oh et al., 2020).

Temperature observations were collected from an extensive network of observatories (i.e., 54 automatic weather stations) spread across Seoul city. The automatic weather stations (AWSs) record air temperatures within a range of -40°C to 60°C with a ± 0.3°C accuracy using a metallic system equipped with thin film sensors. The Korea Meteorological Administration (KMA) provides the ambient air temperature data recorded from AWSs (Korea Meteorological Administration n.d). In the present study, hourly outdoor air temperature was collected from the 54 AWS in Seoul and one rural station in Neunggok over a seven-year period to ensure the spatial and temporal resolutions of our data set; the total number of hourly temperature observations was 3215310 entries. The geographical location of each weather station in Seoul is provided in the supplemental information (see Figure S1).

Calculating urban heat island intensity

UHI is quantified as the outdoor air temperature difference between urban and rural areas (Guattari et al., 2018; Lee et al., 2016; Li et al., 2014). To ensure a proper selection of the reference station, we followed guidelines dictated by the World Meteorological Organization (WMO) (Oke, 2004). The WMO dictates that reference stations for UHI intensity (UHII) computations be located in a relatively flat area with rural characteristics (i.e., vegetated areas with a low building density). Accordingly, we selected Neunggok station as our reference station (i.e., rural station). Neunggok is located in the southern part of Seoul and is located in a flat terrain with a paucity of large buildings and general infrastructure. Moreover, the use of

Neunggok as a reference station is consistent with previous UHI-related studies in Seoul (Lee et al., 2016; Ngarambe et al., 2021; Oh et al., 2020). UHII is calculated using the following equation:

$$UHII = T_{urban} - T_{rural} \quad \text{(Equation 1)}$$

where UHII is urban heat island intensity, T(urban) is the temperature of an urban area, and T(rural) is the temperature of a representative rural area. Average UHII was computed by averaging all UHII values in each month. To effectively quantify the potential effect of UHI on building energy consumption, we considered various temporal UHII indicators (i.e., average UHII, average daytime UHII, and average nighttime UHII). Average daytime UHII and average nighttime UHII were calculated based on the real sunrise and sunset time in Seoul (2011-2017) (Time and date AS, 1995).

Building information and functions

We considered two types of buildings: (I) class 1 residential neighborhood facilities and (II) class 2 residential neighborhood facilities. The Korean government categorizes these buildings based on their sizes. As described in the national law information center run by the Ministry of Government Legislation (Ministry of Government Legislation, 1997), the allowed floor area for class 1 residential neighborhood facilities is less than 1000 m^2 and for class 2 residential neighborhood facilities is less than 500 m^2. Both types of facilities include multi-living facilities (i.e., retail stores, restaurants, bakery, etc.), religious facilities (i.e., churches, temples, prayer centers, etc.), and local government centers (i.e., fire stations, post offices, etc.). We collected the building information such as location, building type, and floor area from the National Geospatial Information Portal run by the Ministry of Land, Infrastructure, and Transport (MOLIT) (Ministry of Land, Infrastructure and Transport, n.d.).

We consider all class 1 and class 2 residential neighborhood facilities within a 200 m radius of each of the 54 AWS. The choice of the radius is based on longest distance where microclimatic influences measured at the AWSs are likely to prevail/extend; the influences of AWS-recorded weather elements are likely to diminish beyond a 200 m radius (Runnalls and Oke, 2006; Stewart and Oke, 2010.). To identify buildings in close proximity to the installed AWS (i.e., within a 200 m radius), we used ArcGIS software; we found a total of 1487 buildings (i.e., 726 class 1 residential neighborhood facilities and 761 class 2 residential neighborhood facilities), and their energy use profiles were subsequently obtained.

Cooling and heating energy consumption data

The Korean government records and publicly avails monthly gas and electric energy consumption of buildings in Seoul via an extensive online repository (Korea Information Society Agency n.d). We used data from the said database to estimate gas and electric energy consumption for heating and cooling purposes. However, the original data provided via the online repository includes total monthly and electric energy inclusive of energy used for other purposes so that it needs segregation to identify electric and gas energy used for cooling and heating purposes alone. In principle, there are various methods to identify building energy use for specific purposes and are extensively discussed by Wang et al. (2012). For simplification, however, the algorithms used can be categorized into two groups: (I) estimation algorithms and (II) disaggregation algorithms. The estimation approach involves calculating individual energy use based on available information such as space use profiles, building type, etc., summing it up and using already available metered energy to validate the calculated energy. While this method has been employed in various studies previously (Cohen et al., 2001; Field et al., 1997), it is susceptible to large uncertainties associated with calculating/estimating individual energy usage for individual components of the space (Wang et al., 2012).

Consequently, we employed the disaggregation method, which segregates total energy consumption into energy use by specific components based on a short-term measurement method (STM) developed by Robison (1992). In the STM method, the total energy is divided into seasonal-varying energy use, which predominantly consists of the energy used for heating and cooling purposes (i.e., heating, ventilation, and air conditioning energy use) and the non-seasonal varying energy use, which includes the steady-state energy consumed regardless of the season (e.g., for lighting or cooking purposes). It is essentially less exhaustive to determine non-seasonal varying energy because it is constant. After determining the non-seasonal varying energy use, seasonal-varying energy is subsequently obtained as the difference between the available in situ total energy and the non-seasonal varying energy use. In our case, the non-seasonal varying energy use was determined as the lowest monthly gas consumption (G_l)/ lowest monthly electric energy

consumption (E_I) in a given year. We assumed such energy to be the steady-state gas/electric energy used for cooking, lighting, appliances, etc. and therefore consistent regardless of the season.

Moreover, the governmental repository database from which our energy consumption data were obtained does not provide information about the cooling/ heating equipment types in each building. We thus could not directly determine the dominant cooling/ heating energy source (e.g., electricity or gas) per building. As such, based on Figure S2 in the supplemental information, which shows high electricity usage during the cooling period (June – September) and similarly heightened gas usage during the heating period (October – March), electricity was considered the dominant energy source for cooling purposes while gas energy was considered the dominant energy source for heating purposes. Finally, the monthly seasonal varying energy use, which in our case equated to monthly cooling/heating energy use, was determined as the difference between monthly total electric energy consumption ($E_{total\_monthly}$)/monthly gas energy consumption $G_{total\_monthly}$) and E_I/G_I as shown in Equations 2 and 3, and this approach has been employed in several previous studies (Ahn et al., 2019; Li et al., 2014).

Cooling season,

$$C_{monthly} = E_{total\_monthly} - E_I \quad \text{(Equation 2)}$$

Heating season,

$$H_{monthly} = G_{total\_monthly} - G_I \quad \text{(Equation 3)}$$

where $C_{monthly}$ is the monthly cooling energy consumption, $E_{total\_monthly}$ is the total monthly electric energy consumption, E_I is the non-seasonal varying electric energy use, $H_{monthly}$ is the monthly heating energy consumption, $G_{total\_monthly}$ is the total monthly gas energy consumption, and G_I is the non-seasonal varying gas energy use. Building energy consumption patterns between class 1 and class 2 residential neighborhood facilities are shown in the supplemental information (Figures S3–S5).

Computing CDDs and HDDs

The CDDs and HDDs are commonly used in analyzing the weather-sensitive building energy consumption for cooling and heating seasons. We calculated the CDD and HDD using the following equations:

$$CDD = \sum_{i=1}^{N} (T_i - T_b) \ (for\ T_i \geq T_b) \quad \text{(Equation 4)}$$

$$HDD = \sum_{i=1}^{n} (T_b - T_i) \ (for\ T_i \leq T_b) \quad \text{(Equation 5)}$$

T_i is the mean temperature of the day i, T_b is the base temperature, and N and n are the numbers of the days when the mean daily temperature is above and below the base temperature, respectively. The base temperature is defined as the ambient air temperature at which no heating or cooling is needed (ASHRAE, 2001). It can be different according to locations. For example, the base temperature to calculate CDDs and HDDs in the United States, United Kingdom, and Germany is 18.3°C, 15.5°C, and 15°C, respectively (Lee et al., 2014). In this study, in the case of South Korea, we used 26°C as the base temperature for calculating CDDs and 18°C for HDDs according to Choi (2005).

The HDDs and CDDs computed for the urban area are compared to those computed for the rural reference area to obtain an estimate of the energy use differences between the urban and rural building stocks. Ideally, the cooling and heating energy data of urban building and rural building stocks should be computed and compared for such an assessment. However, considering that our designated rural area contained a limited number of buildings, it was somewhat challenging to obtain a substantial amount of data for comparison with the energy consumption from the urban building stock. Consequently, we use the HDD/CDD values as proxies for energy use.

QUANTIFICATION AND STATISTICAL ANALYSIS

To explore the relationship between UHII, outdoor air temperature, and building energy consumption while minimizing the influence of errors and noise in our data set, we binned the UHII data and outdoor air temperature data into several categories. The bin widths were 0.5°C for UHII, 1°C for outdoor air temperature, 10°C for CDDs, and 40°C for HDDs. For the cooling season, we had 10 average UHII bins, 12

average nighttime UHII bins, and 9 average daytime UHII bins for class 1 residential neighborhood facilities and 10 average UHII bins, 12 average nighttime UHII bins, and 8 average daytime UHII bins for class 2 residential neighborhood facilities. For the heating season, we had 10 average UHII bins, 11 average nighttime UHII bins, and 10 average daytime UHII bins for class 1 residential neighborhood facilities and 10 average UHII bins, 10 average nighttime UHII bins, and 9 average daytime UHII bins for class 2 residential neighborhood facilities. The case count for each bin is presented in the supplemental information (see Table S1 and S2), and the equality of variances between the bins was estimated using the Levene's test of equal variance (Gastwirth et al., 2009); these results are also presented in the supplemental information (see Table S3). Also, we had 11 temperature bins for cooling season, 26 temperature bins for heating season, 14 CDD bins, and 20 HDD bins. We then studied the variance in mean building energy consumption among the said binned groups. To ensure that the mean differences in building energy consumption across UHII and temperature groups were statistically significant, we conducted a Kruskal-Wallis analysis mainly because our data violated several assumptions required to employ parametric statistical tests such as analysis of variance. The Kruskal-Wallis analysis is approximated via the statistical equation below:

$$H = \frac{12}{N(N+1)} + \sum_{i=1}^{k} \frac{R_i^2}{n_i} - 3(N+1) \qquad \text{(Equation 4)}$$

where,

N = sum of the sample sizes for all samples

k = number of samples

n = size of the i^{th} sample

R_i = sum of the ranks in the i^{th} sample